Thermal Decomposition of Cyclotriphosphazenes. I. Alkyl–Aminoaryl Ethers

S. V. LEVCHIK,[1,*] G. CAMINO,[1] M. P. LUDA,[1] L. COSTA,[1] A. LINDSAY,[2] D. STEVENSON[2]

[1] Dipartimento di Chimica Inorganica, Chimica Fisica e Chimica dei Materiali dell'Università, Via P. Giuria 7, 10125 Torino, Italy

[2] 3M Harlow Research Ltd., Pinnacles, Harlow Essex, CM 195AE, United Kingdom

Received 16 April 1997; accepted 10 June 1997

ABSTRACT: 1,3,5 - Triisopropoxy–1,3,5 - tris(4 - aminophenoxy)–cyclotriphosphazene-[CTP (I)], 1,3,5 - trineopentoxy–1,3,5 - tris(4 - aminophenoxy)–cyclotriphosphazene [CTP (II)], and 1,1,3,5-tetraneopentoxy–3,5-bis(4-aminophenoxy)–cyclotriphosphazene [CTP (III)] were prepared from hexachlorotricylophosphazene. Thermal decomposition of the crude CTP (I), CTP (II), and CTP (III) was studied by thermogravimetry, differential scanning calorimetry, and thermal volatilization analysis. Solid, gaseous, and high boiling degradation products were collected at different steps of thermal decomposition and identified by using infrared and gas chromatography mass spectrometry. On heating to 600°C, CTP (I) shows three main steps of weight loss, whereas both CTP (II) and CTP (III) show two overlapping steps. The first step of thermal decomposition of CTP (I) is observed at 150–200°C, where elimination of part of the aliphatic substituents and polymerization of the CTP (I) occurs. The opening of tricyclophosphazene rings at 220–370°C provokes further elimination of aliphatics and ammonia and formation of crosslinked structures. Phosphorus oxynitride structure bonded with carbonized polyaromatics is formed in the third step of thermal decomposition, accompanied by the elimination of aromatics and chain fragments at 400–500°C. In the case of CTP (II) and (III), simultaneous evaporation of virgin CTPs, opening of the phosphazene ring, and elimination of aliphatic substituents with the formation of crosslinked polymeric structures occur at 210–350°C. A phosphorus oxynitride–aromatic carbonized structure similar to that from CTP (I) is formed at 350–600°C. The process is accompanied by the elimination of aromatics and chain fragments.
© 1998 John Wiley & Sons, Inc. J Appl Polym Sci **67:** 461–472, 1998

INTRODUCTION

Cyclotriphosphazenes (CTPs) are of great interest in both material research[1–4] and application[5–8] because they are used as monomers for high performance linear, cyclolinear, and cyclomatrix polymers.[1,2,6] When CTPs are incorporated into the network of thermosetting polymers or in the chain structure of thermoplastics, they can increase the thermal and/or fire resistance of the polymers.[8,9–17] Mechanistic studies of CTPs' thermal decomposition reported in the literature[1,2] are mostly limited to investigations of ring opening and ring size equilibration, which are important in the polymerization of CTPs.

In this article, the synthesis and the mechanistic study of thermal decomposition behavior of three nongeminal alkyl–aminoaryl ethers of cyclotriphosphazene are reported.

* *Permanent address:* Research Institute for Physical Chemical Problems, Byelorussian State University, Leningradaskaya, 14, Minsk-220080, Belarus.

Correspondence to: G. Camino.

Journal of Applied Polymer Science, Vol. 67, 461–472 (1998)
© 1998 John Wiley & Sons, Inc. CCC 0021-8995/98/030461-12

EXPERIMENTAL

Materials

1,3,5-Triisopropoxy–1,3,5-Tris(4-aminophenoxy)–Cyclotriphosphazene [*CTP (I)*]

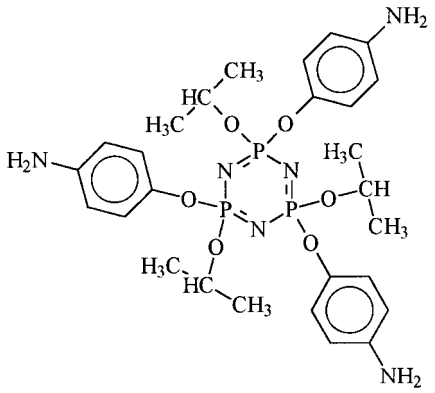

I

The synthesis was carried out as described in Bezoari.[18] A mixture of sodium isopropoxide (0.15 mol) in anhydrous tetrahydrofuran (100 mL) was added dropwise to a stirred solution of hexachlorocyclotriphosphazene (17.25 g, 0.05 mol) in dry tetrahydrofuran (100 mL) under nitrogen atmosphere. The mixture was refluxed for 5 h and allowed to cool. A slurry of sodium 4-aminophenoxide (0.15 mol) in anhydrous tetrahydrofuran (250 ml) was added, and the mixture refluxed for 90 h. The mixture was then allowed to cool, and water (250 mL) was added. The separated organic layer was evaporated to give a dark brown oil. After stirring with petroleum spirit (bp = 40–60°C), a dark brown powder is precipitated. The product was filtered off and dried under vacuum over phosphorus pentoxide. The yield was 27.6 g (87%).

1,3,5-Trineopentoxy–1,3,5 Tris(4-aminophenoxy)–Cyclotriphosphazene [*CTP (II)*]

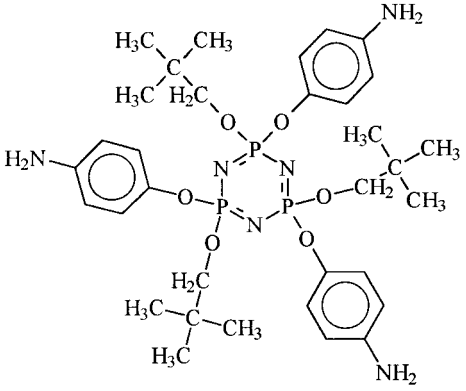

II

Sodium neopentoxide (0.173 mol) in anhydrous tetrahydrofuran (100 mL) was added over 30 min to a stirred mixture of hexachlorocyclotriphosphazene (20 g, 0.057 mol) in anhydrous tetrahydrofuran (100 mL) under nitrogen. The reaction temperature reached 50°C and was maintained at this temperature for 18 h, then it was refluxed for 5 h. The mixture was allowed to cool, and a slurry of sodium 4-aminophenoxide (0.173 mol) in anhydrous tetrahydrofuran (100 mL) was added. The reaction mixture was then refluxed for 42 h, the solvent removed, and the residue partitioned between ether and water. The ether layer was dried over sodium sulphate and evaporated to give a dark brown tar, which was triturated with petroleum spirit (bp = 40–60°C) to give a pale brown solid, which was dried under vacuum over phosphorus pentoxide. The yield was 27.6 g (71%).

1,1,3,5-Tetraneopentoxy–3,5-bis(4-Aminophenoxy)–Cyclotriphosphazene [*CTP (III)*]

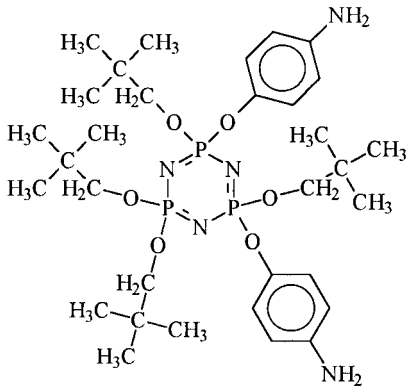

III

Sodium neopentoxide (0.23 mol) in anhydrous tetrahydrofuran (150 mL) was added dropwise to a stirred solution of hexachlorocyclotriphosphazene (20 g, 0.057 mol) in anhydrous tetrahydrofuran (200 mL) under a nitrogen atmosphere. The mixture was refluxed for 18 h and allowed to cool, and a slurry of sodium 4-aminophenoxide (0.114 mol) in anhydrous tetrahydrofuran (200 mL) was added. The mixture was refluxed for 140 h, then the solvent was evaporated to give a dark brown oil. This was dissolved in ethyl acetate (500 mL), and the solution washed with water (3 × 200 mL), dried over sodium sulphate, and evaporated to give a black tar. The tar was washed and stirred with petroleum spirit (bp = 40–60°C) (5 × 250 mL) and then was heated under vacuum until solidified. This solid was hand-ground to give a brown powder. The yield was 15.3 g (38%).

Table I Chemical Shifts for Substituted Cyclotriphosphazenes

CTP (I)		CTP (II)		CTP (III)	
δ (ppm)	Signal[a]	δ (ppm)	Signal	δ (ppm)	Signal
^{1}H-NMR					
6.9–6.4	m.	6.9–6.6	m.	6.9–6.4	s.m.
	—	6.5–6.3	m.	—	—
4.9	b.s.	4.9	b.s.	—	—
4.6–3.8	s.m.	3.6–2.8	s.m.	3.6	m.
1.3–0.9	m.	0.9–0.7	m.	0.9	m.
^{13}C-NMR					
145	s.s.	145	s.s.	146	triplet
141	s.s.	140	s.s.	141	doublet
121	—	121	s.s.	122–121	s.s.
114	—	114	s.s.	115	—
70	s.s.	76	s.s.	75	—
		34–31	s.s.	32	s.s.
23	—	26	s.s.	26	—
^{31}P–NMR					
23.5	triplet	26.5	m.	—	—
	—	25.5	m.	—	—
15–9	s.s. (minor)	16–8	s.s. (minor)	—	—
	—	14	doublet	—	—
	—	13.7	singlet	—	—
	—	11	doublet	—	—

[a] m = multiplet; s.m. = several multiplets; b.s. = broad singlet; s.s. = several signals.

Characterization

The cyclotriphosphazenes CTP I, II, and III were not further purified; and the thermal degradation was carried out on the crude products. Indeed, contaminants are likely to be due to a sustitution pattern ot the cyclotriphosphazene ring with a different balance between alkoxy and phenoxy groups or to a residual traces of chlorine atoms, which, however, are not relevant to the mechanism of thermal degradation and phosphazene ring evolution to a thermally stable char, which is the main purpose of this article and does not depend on these structural differences, as shown below.

^{1}H, ^{13}C, and ^{31}P chemical shifts and main infrared (IR) absorptions and their attribution of CTPs are listed in the Tables I and II, respectively.

Thermal Analysis

The thermal decomposition of the CTPs was studied at a heating rate of 10°C min under nitrogen flow (60 cm^3/min) by thermogravimetry (TG) and differential scanning calorimetry (DSC), by using a Du Pont 2100 thermal analyzer provided with DSC and TGA 2950 (high resolution) modules or under dynamic vacuum (10^{-3}–10^{-4} mm Hg) by thermal volatilization analysis (TVA), by using homemade equipment.[27] The sample pans used were made of aluminium in TG and DSC and glass in TVA.

TG was carried out in the high-resolution mode (HRTG), in which the resolution of overlapping processes is improved by decreasing the heating rate when the rate of weight loss, as monitored by derivative TG, tends to increase. Several settings in the range of 0 ÷ +10 are available to control the resolution. The setting +5 was used in our experiments. In these conditions, the temperature at which phenomena occur is lower than on constant heating at 10°C/min.

On heating under vacuum, CTPs' degradation competes with volatilization, which is suppressed by preheating at 10°C/min under nitrogen to 200°C (CTP I) or 320°C (CTP II and III) in the TVA apparatus prior to degradation under vacuum because of partial self-condensation taking place at these temperatures, as shown below.

Table II Attribution of the Main Infrared Absorptions of CTP (I), (II), and (III)

Absorptions (cm^{-1})				
CTP (I)	CTP (II)	CTP (III)	Attribution	References
3454	3435	3456	ν_{as} (N—H)	19
3352	3384	3356	ν_{s} (N—H)	19
3225	3227	3225	ν (N—H, hydrogen-bonded)	19
2979	2958	2958	ν_{as} (C—H, of CH_3)	19
2933	2930	2939	ν (C—H of CH—O)	19
2870	2870	2871	ν_{s} (C—H, of CH_3)	19
1628	1626	1624	ν (Φ, quadrant) and δ (NH_2)	19
1511	1509	1510	ν (Φ, semicircle)	19
1251	1254	1252	ν (P═N)	1, 21–26
1182	1183	1184	ν (P═N)	1, 21–26
1165	1162	1164	ν (P═N)	1, 21–26
1111	1076	1076	ν (Φ—OP)	19, 20, 26
1014	1029	1029	ν (C—OP)	19, 20, 26
961	972	974	ν (P—OΦ)	19, 20, 26
833	834	835	ν (P—OC)	19, 20, 26

Degradation Products

Solid degradation products were collected in thermogravimetry at the end of each step of thermal decomposition of the CTPs. High boiling products (HBP) condensable at room temperature were collected on the water-cooled glass finger introduced inside the glass cylinder[28] used for CTPs' degradation in TVA experiments under vacuum. Gases evolved on thermal decomposition were trapped by liquid nitrogen in the TVA apparatus. To separate overlapping processes of volatilization, preheated CTPs were heated in TVA at 10°C/min to the temperature of the beginning of gas evolution of the step under study and left at this temperature until the gas evolution is completed. The identification of the degradation products was carried out either by IR (Perkin–Elmer 2000 FTIR) or by gas chromatography mass spectrometry (Hewlett Packard 5970B).

RESULTS

Thermal Decomposition

Thermogravimetry

In spite of the similarity of the chemical structures, CTP (I) has a very different behaviour in HRTG as compared to CTP (II) and CTP (III) (Fig. 1). CTP (I) shows the onset of weight loss at a rather low temperature (110°C) and three steps of weight loss [Fig. 1, curve (a)] with maxima of the rate at 160, 264, and 422°C [Fig. 1, curve (a′)]. Both CTP (II) and (III) show the onset of weight loss at 170°C [Fig. 1, curves (b) and (c)], two overlapping degradation steps at about 210 and 230°C and almost constant rate of weight loss at 250–600°C [Fig. 1, curves (b′) and (c′)]. CTP (I) leaves a larger residue at 600°C (65%) than CTP (II) (54%) and CTP (III) (50%).

Differential Scanning Calorimetry

CTP (I) shows three major peaks: two exotherms at 203 and 468°C, and an endotherm at 318°C [Fig. 2, curve (a)]. A small exothermal peak at 340°C overlaps with the endothermal peak at 318°C. The major thermal effects correspond to the three steps of weight loss observed in HRTG [Fig. 1, curve (a)]. The discrepancy between the temperatures of DSC and derivative TG peaks is due to different heating programs used.

Both CTP (II) and CTP (III) show complex but similar behaviour in DSC [Fig. 2, curves (b) and (c)]. Two relatively weak endothermal processes are observed at 90–140°C, which are likely to be due to solid–solid phase transitions. Evaporation occurs at 252–263°C, as shown by crystals of virgin CTP (II) or CTP (III) found on the cover of DSC cell when the experiments were interrupted at these temperatures. The endothermal peaks at 290–294°C overlapping with exotherms at 300–307°C

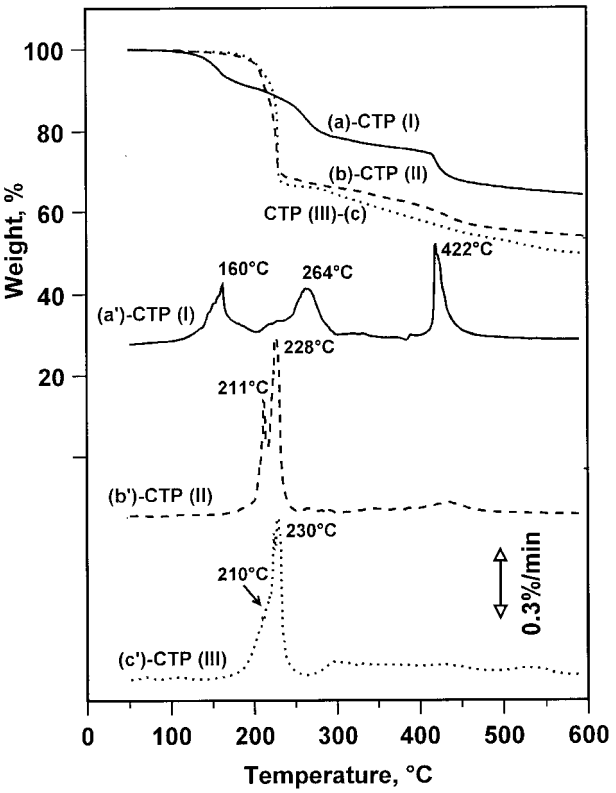

Figure 1 High-resolution thermogravimetry (a)–(c) and derivative curves (a′)–(c′) of (a) and (a′) CTP (I), (b) and (b′) CTP (II), and (c) and (c′) CTP (III). The heating rate is 10°C min; the resolution setting is +5; the nitrogen flow is 60 cm^3/min.

should be due to thermal decomposition. It is likely that the thermal effects at 250–310°C [Fig. 2, curves (b) and (c)] correspond to the two overlapping steps of weight loss at 210–230°C in HRTG [Fig. 1, curves (b′) and (c′)], whereas exotherms at 320–600°C [Fig. 2, curves (b) and (c)] correspond to the interval of constant weight loss at 250–600°C in HRTG [Fig. 1, curves (b′) and (c′)].

Thermal Volatilization Analysis

Preheated CTP (I) shows three maxima of total gas evolution at 200, 295, and 450°C [Fig. 3(a), solid line], which might be tentatively attributed to the three steps of weight loss in HRTG [Fig. 1, curves (a) and (a′)]. Both preheated CTP (II) and CTP (III) show similar curves with maxima at 365 and 450°C [Fig. 3(b) and (c), solid lines], which is likely to occur in the region of constant weight loss in HRTG [Fig. 1, curves (b), (b′), (c), and (c′); $T >$ 250°C]; whereas little gaseous products are formed below 250°C, which are eliminated in the pre-heating treatment. This is in contrast with CTP (I), which shows the first step of gases evolution (200°C) in spite of the preheating. For all CTPs under study, noncondensable gases evolve in two steps, as follows: slowly at 445–450°C, and with a higher rate at 535–540°C (Fig. 3, dashed lines).

Products of Degradation

Gases and high boiling products of decomposition were collected in TVA from the preheated CTPs, whereas solid residues were collected in HRTG from the decomposition of virgin CTPs.

Gases

The gaseous products collected from isothermal decomposition of preheated CTP (I), CTP (II), and CTP (III) are shown in the Tables III and IV, respectively.

High Boiling Products and Solid Residue

In the residue of the first step of weight loss of CTP (I) [10% at 200°C; Fig. 1, curve (a)], two

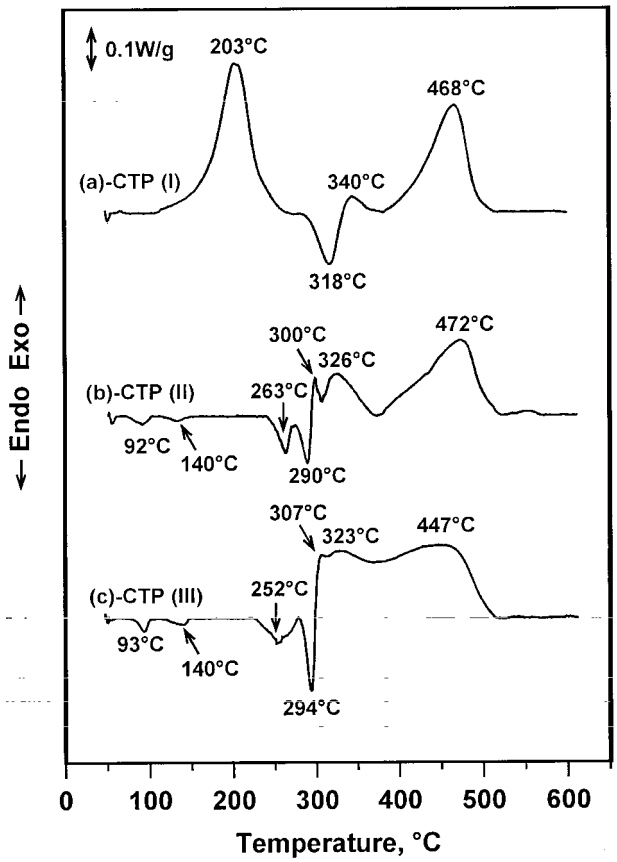

Figure 2 Differential scanning calorimetry curves of (a) CTP (I), (b) CTP (II), and (c) CTP (III). The heating rate is 10°C/min; the nitrogen flow is 60 cm^3/min.

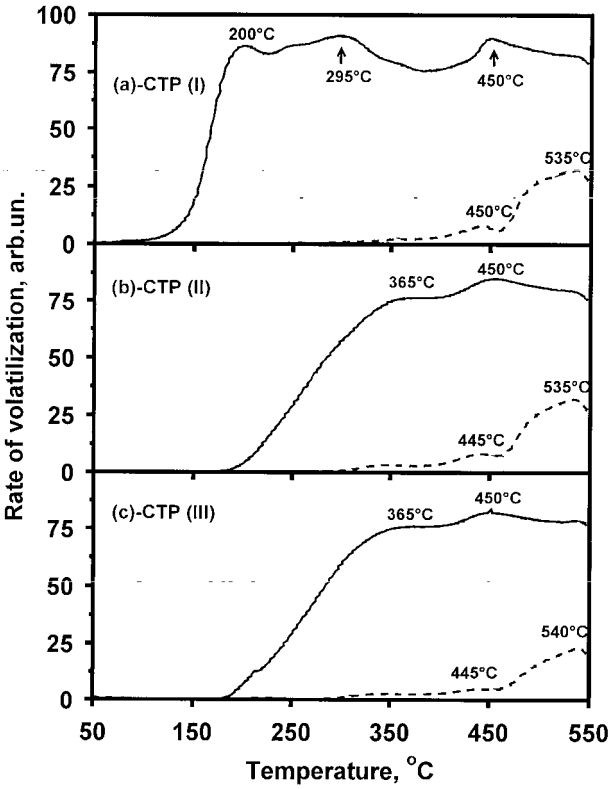

Figure 3 Thermal volatilization analysis curves of pre-heated (a) CTP (I), (b) CTP (II), and (c) CTP (III). Solid lines represent total gases; dashed lines represent gases noncondensable at −196°C. The heating rate is 10°C/min; the dynamic vacuum is 10^{-3}–10^{-4} mm Hg.

absorptions of ν (P═N) at 1251 and 1182 cm^{-1} [Fig. 4, spectrum (a); Table II] shift to higher wave numbers [1289 and 1200 cm^{-1}, respectively; Fig. 4, spectrum (b)], which might be due to the modification of the chemical structure of the substituents.[1] A new broad band at 923 cm^{-1} [Fig. 4, spectrum (b)] overlapping with ν (C—OP) at 961 cm^{-1} [Fig. 4, spectrum (a)] is attributed to ν (P—OP).[19,20] The variation of intensity and position of ν (N—H) at 3454, 3352, and 3225 cm^{-1} and δ (NH_2) 1628 cm^{-1} [Fig. 4, spectra (a) and (b); Table II] might be due to distortion of the hydrogen-bonding network.[19]

Table III Gaseous Products of Thermal Decomposition of Preheated CTP

T (°C)	Volatiles
200	Cyclopropane, propene, ammonia (traces), water
290	Cyclopropane, propene, ammonia, water
440	Benzene, ammonia, aniline, cyclopropane, propene, various aliphatic hydrocarbons
560	Benzene, ammonia, aniline

Table IV Gaseous Products of Thermal Decomposition of Preheated CTP (II) and CTP (III)

T (°C)	Volatiles
340	1,1-Dimethylcyclopropane, 2-methyl-2-butene, ammonia, water (traces)
430	Ammonia, 1,1-dimethylcyclopropane, 2-methyl-2-butene, 2-methylpropene, benzene, aniline
560	Benzene, aniline, ammonia

Similar modifications of the IR pattern [Fig. 4, spectra (a) and (b)] are observed in the first step of weight loss (30%) of CTP (II) at 250°C [Fig. 5, spectra (a) and (b)]. Because for CTP (II) and CTP (III), the thermal decomposition behavior as followed by IR of solid residues and HBP is similar, the IR characterization of CTP (II) only will be discussed below.

In the first step of weight loss, crystals of volatilized virgin CTP (II) and CTP (III) were found on the cooled part of thermobalance in HRTG, but not in the case of CTP (I). This indicates that self-condensation (see below) competes with volatilization of unaltered CTP (II) and CTP (III).

The IR spectrum of the solid residue of CTP (I) is strongly modified in the second step of weight loss [12% at 300°C; Fig. 1, curve (a)]. Decreasing of the C—H stretching of aliphatics at 3000–2800 cm^{-1} [Fig. 4, spectra (b) and (c)] corresponds to the extensive elimination of the aliphatic substituent (Table III). Decreasing of the intensity of the absorption at 1507 cm^{-1} (ν Φ semicircle), in which the extinction coefficient is known to be enhanced by electron donor substituents such as NH_2, is due to the involvement of this group in a chemical reaction (see below). Indeed, ammonia is found among volatiles evolved (Table III). Instead of the two ν (P═N) bands at 1289 and 1200 cm^{-1} in Figure 4, spectrum (b), a broad absorption at 1231 cm^{-1} is observed in Figure 4, spectrum (c), which might be caused by the opening of the phosphazene ring.[1,2,21,29–31] The occurrence of secondary rearrangement reactions such as alkoxyphosphazene–oxophosphazene rearrangement leading to phosphoryl functionalities,[1,22–24,32] also absorbing at 1231 cm^{-1}, cannot be excluded.

Volatilization of high boiling products, together with gases observed for CTP (I) in TVA at 440°C,

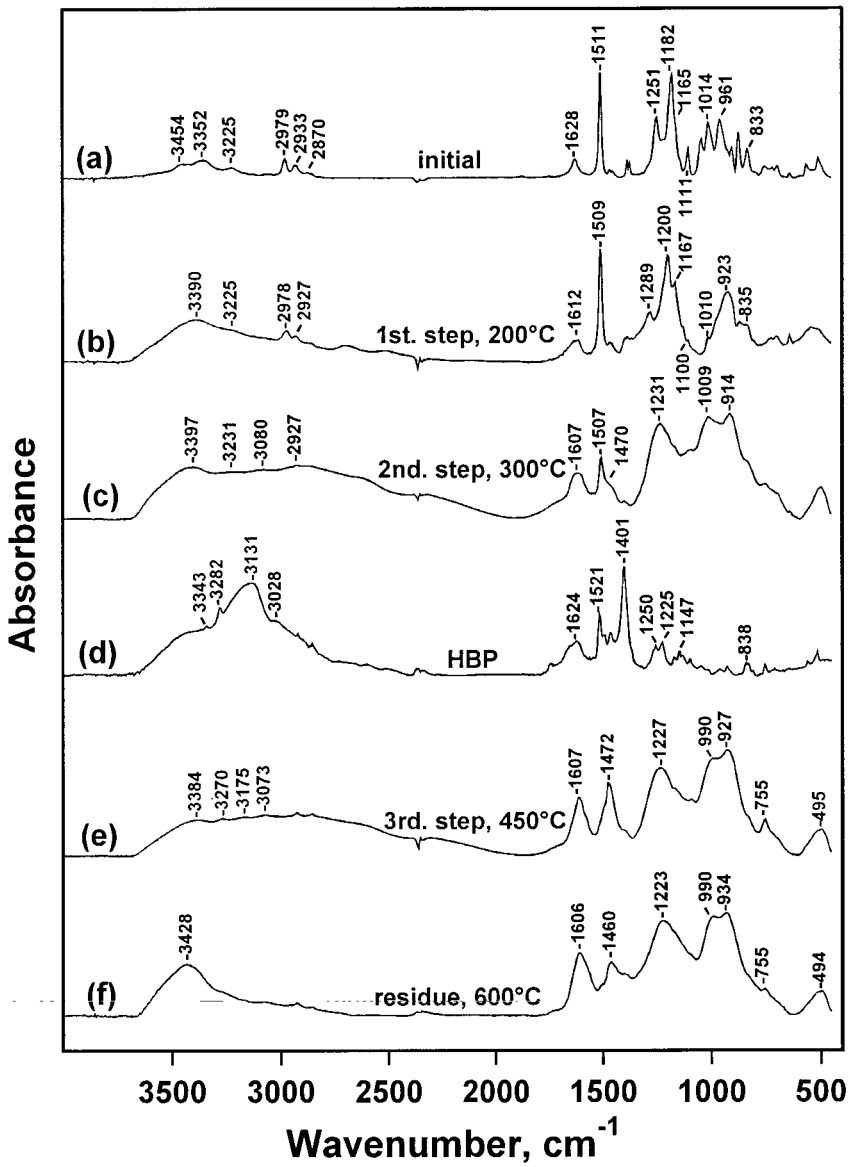

Figure 4 Infrared spectra of (a) CTP (I). Residues collected in HRTG on heating at 10°C/min are as follows: (b) after the first step of weight loss at 200°C, (c) after the second step of weight loss at 300°C, (e) after the third step of weight loss at 450°C, and (f) at 600°C. (d) High boiling products collected in TVA at 440°C. Pellets in KBr.

occurs in the third step of weight loss of HRTG [Fig. 1, curve (a)]. The HBP contain ammonium cations (NH_4^+) detected by the strong characteristic absorptions at 3131 [ν (N—H)] and 1401 cm^{-1} [δ (NH_4^+)] and aromatic amines detected by ν (N—H) at 3343 and 3282 cm^{-1}, ν (CH, Φ) at 3028 cm^{-1}, δ (NH) and ν (Φ, semicircle) at 1624 cm^{-1}, ν (Φ, quadrant) at 1521 cm^{-1}, and δ (CH, Φ) at 838 cm^{-1} [Fig. 4, spectrum (d)]. Phosphorus-containing species show a series of weak bands at 1300–1100 cm^{-1}. Thus, the HBP are likely to consist of ammonium salt of phosphorous and aromatic-amines-containing species.

The modifications of the IR pattern of CTP (I) observed in the second step proceed also in the third step at 450°C [Fig. 4, spectrum (e)]. The high frequency ν (Φ, quadrant) at 1507 cm^{-1} disappear in the spectrum [Fig. 4, (e)], probably because of complete consumption of NH_2 groups. The absorption at 1472 cm^{-1} appearing first in the second step [shoulder at 1470 cm^{-1}; Fig. 4, spectrum (c)] and growing in the third might be attributed to the

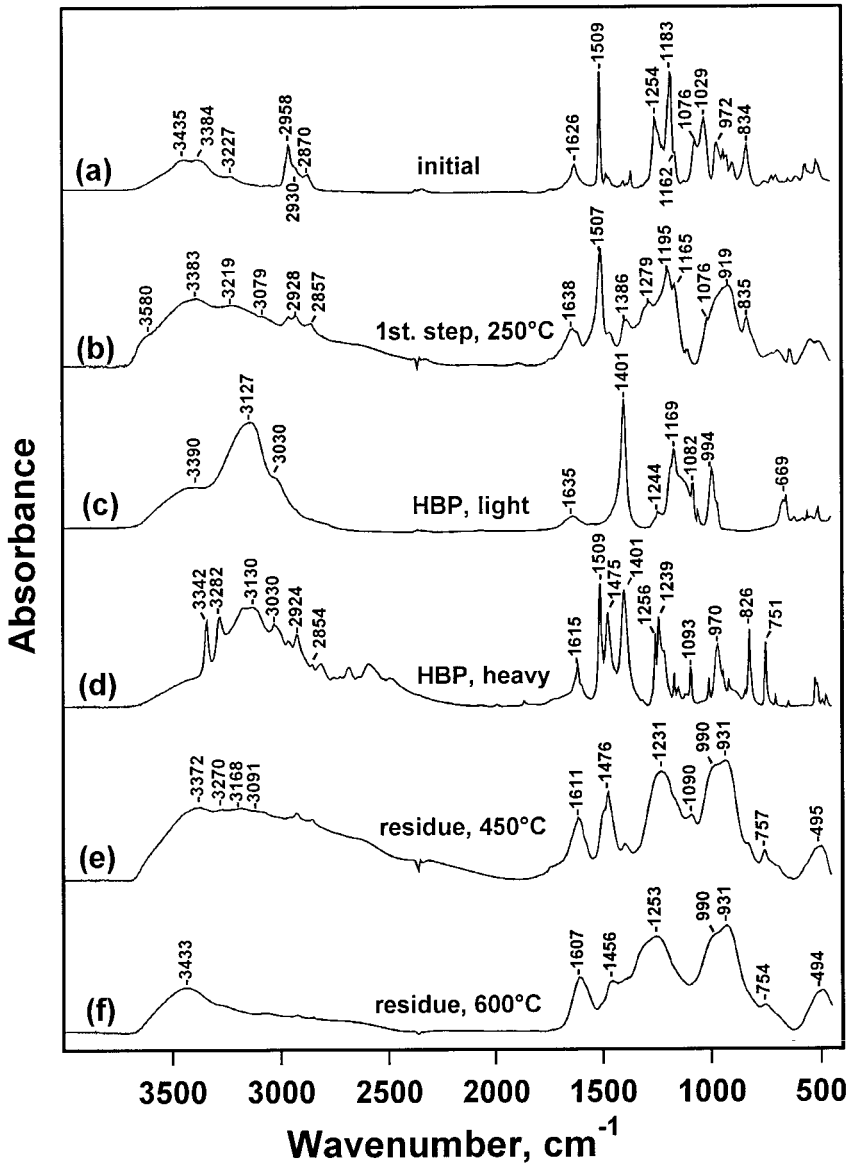

Figure 5 FTIR spectra of (a) CTP (II). Residues collected in HRTG on heating at 10°C/min are as follows: (b) after the first step of weight loss at 250°C, (e) at 450°C, and (f) at 600°C. (c) Light and (d) heavy fractions of high boiling products collected in TVA at 430°C. Pellets in KBr.

mixed ν (Φ, quadrant) mode[19] where para-, meta-, and ortho- substituents contribute.

CTP (II) shows similar evolution of the IR spectrum of solid residue [Fig. 5 spectra (b) and (e)] in the region of constant weight loss [Fig. 1, curve (b)] as it was observed for CTP (I) in the second and third steps [Fig. 4, spectra (b), (c), and (e)]. HBP are formed under vacuum in the step of constant rate of thermal decomposition of CTP (II). The HBP are separated into two fractions on the water-cooled glass finger. The lighter fraction of HBP [Fig. 5, spectrum (c)], which was condensed in the higher part of the water-cooled glass finger is likely to consist of ammonium salt (absorptions at 3127 and 1401 cm^{-1}) of phosphorus-containing species (absorptions at 1300–900 cm^{-1}); whereas the heavier fraction of HBP condensed in the lower part of the finger shows a more complex IR pattern [Fig. 5, spectrum (d)]. Absorptions at 3130

and 1401 cm^{-1} are attributed to NH_4^+ as above; absorptions at 3342, 3282, and 1615 (in part) cm^{-1} to NH_2; absorptions at 3030, 1615 (in part), 1509, 1475, 826, and 751 cm^{-1} to aromatics; absorptions at 2924 and 2854 cm^{-1} to aliphatics; absorptions at 1256 and 1239 cm^{-1} to

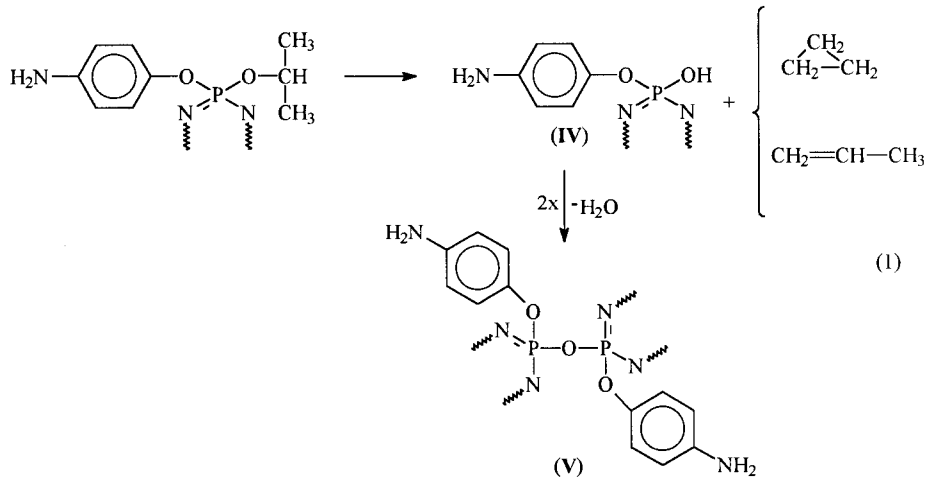

P=N; and absorptions at 1093 and 970 cm^{-1} to P—O—Φ. Since the spectrum of Figure 4 is comparable to the combination of spectra (c) and (d) of Figure 5, it is concluded that similar HBP are evolved from the degrading CTPs. The separation of components of Figure 5 allows,

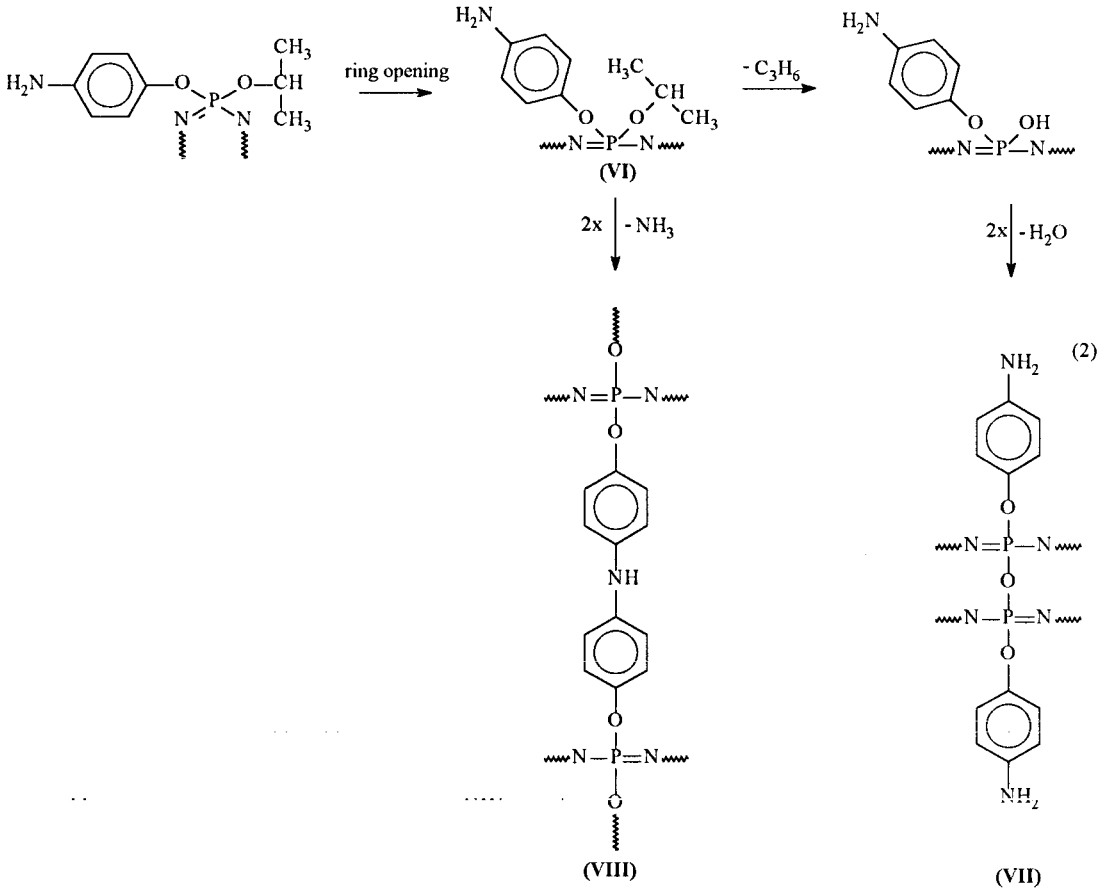

however, more detailed assignments of absorptions, which give better insight of the mechanism of HBP formation. It seems, indeed, that fragments of CTPs bearing acidic functionality volatilize, which are partially neutralized by evolving ammonia since in the broad bands at 2800–2500 cm^{-1} [Fig. 5, spectrum (d)], indicate the presence of unneutralized OH.

The solid residues obtained from CTP (I) and CTP (II) at 600°C are similar [Figs. 4 and 5, spectra (f)]. Disappearance of ν (N—H) at 3300–3000 cm^{-1} on heating to 600°C [Figs. 4 and 5, spectra (e) and (f)] is in correspondence with the evolution of aniline and ammonia. (Tables III and IV). The presence of phenoxyphosphoric ethers in the residues is detected by strong ν (P—OΦ) absorption at 990 cm^{-1} [Figs. 4 and 5, spectra (f)]. The remaining broadbands of aromatics at 1610–1605, 1460–1455, and 750–755 are characteristic bands of carbonized polymers[33]; whereas broad absorptions at 1260–1220 ν (P=N) and 935–930 cm^{-1} ν (P—OP) are typical for phosphorus oxynitrides.[34] Thus, the solid residue at 600°C seems to consist of crosslinked phosphorus oxynitride and carbonized aromatic networks.

No chlorinated species were found either in volatile products or in solid residues, which might indicate that impurities if, any, due to noncomplete substitution of hexachlotricyclophosphazene, are minor.

DEGRADATION MECHANISM

The elimination of the aliphatic substituent in the first reaction occurs on heating CTP (I), as shown by the fact that cyclopropane and propene are the major volatile products formed (Table III).
The resulting hydroxytricyclophosphazene (IV, eq 1) tends to self-condense, evolving water and producing high-molecular-weight compounds (V, eq 1) with P—O—P bridges,[34] which were detected in the IR of solid residue [Fig. 4, spectrum (b)]. The increase in molecular weight apparently slows down the elimination of the isopropyl substituent.

Ring opening (or widening) observed in the second step of degradation is accompanied by further elimination of aliphatic substituents with ensuing condensation and water elimination. Furthermore, in this step also, condensation of NH_2 groups occurs with ammonia evolution (Table III).

The endotherm at 318°C and overlapping exotherm at 340°C in this step [Fig. 2(a)] should correspond to the two condensation processes.

Combination of the two condensation processes leads to a crosslinked structure in which —P=N— chains are either bridged by oxygen atom (VII, eq 2) or by bis(paraminophenoxy) groups (VIII, eq 2). These last partially thermally decompose in the third step of degradation of CTP (I) at 450°C by scission of Φ—N and Φ—O bonds, as shown by the evolution of ammonia, benzene, and aniline (Table III). Phosphorus oxynitride cross-linked structures are likely to be formed (X, eq 3), as follows.

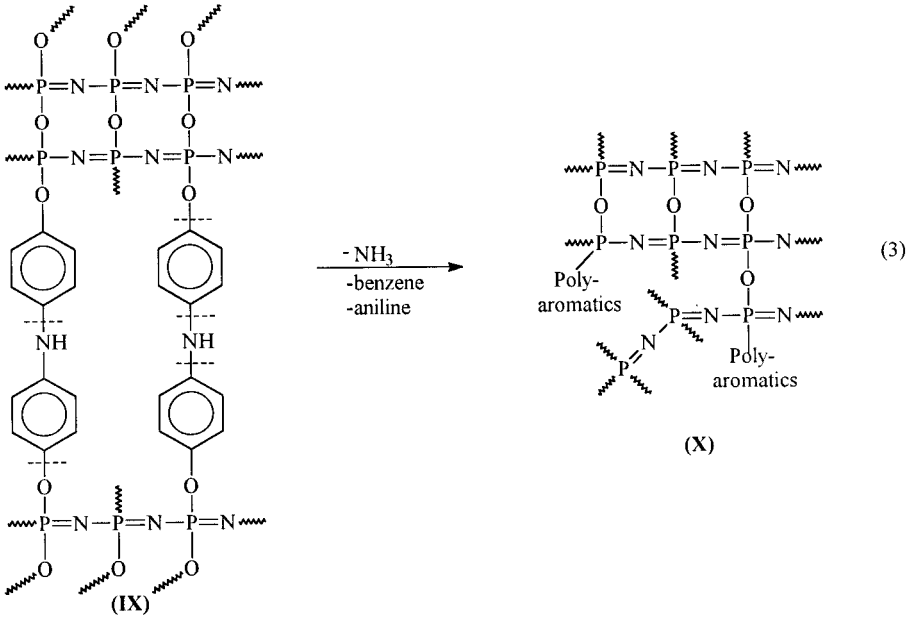

(IX) (X) (3)

The aromatic structures retained in the solid residue undergo carbonization by condensing of benzene rings in the polyaromatic structures. This is in agreement with the evolution of gases noncondensable at −196°C, probably hydrogen, above 450°C in TVA [Fig. 3(a), dashed curve]. The IR absorptions of aromatics at 1607, 1472, and 755 cm^{-1} are also in favor of the carbonization.

The high boiling products detected in this step are fragments of the structure (IX, eq 3) volatilizing upon its transformation to (X, eq 3). The ammonium derivative seen in Figure 4(d) is formed by reaction between —POH groups and ammonia created in the fragmentation process.

The mechanism of thermal decomposition discussed above for CTP (I) is also valid for CTP (II) and CTP (III). However, in the case of CTP (II) and CTP (III), the scission of aliphatic ether bonds is observed at higher temperatures, (>180°C) at which CTPs begin to evaporate. The higher thermal stability of CTP (II) and CTP (III) is probably due to the restriction of hydrogen transfer in neopentoxy substituent because of the presence of quaternary carbon (XI), as follows.

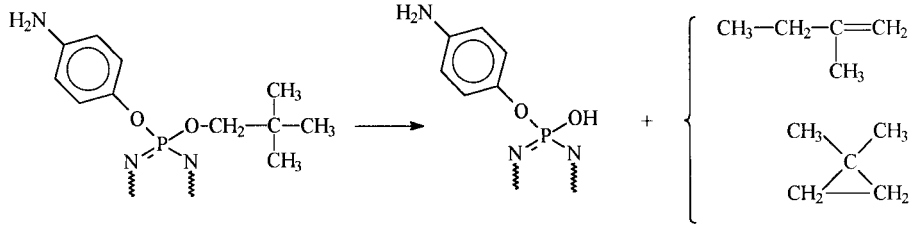

The chemical route to the thermally stable crosslinked phosphorous oxynitride structure is seen to proceed through the elimination of substituents of the phosphazene ring and its opening. Thus, substitution impurities that may be present in the crude materials used in this study do not affect the conclusion, which is of interest to the charring approach in fire-retardant polymer materials.

The authors are most grateful to the EEC for financial support of this work in the frame of the BRITE EURAM project (contract BREU-CT91-0466).

REFERENCES

1. H. R. Allcock, *Chem. Rev.,* **72,** 315 (1972).
2. R. H. Neilson and P. Wisian-Neilson, *Chem. Rev.,* **88,** 541 (1988).
3. C. H. Allen, *Chem. Rev.,* **91,** 119 (1991).
4. D. E. C. Corbridge, *Phosphorus. An Outline of its Chemistry, Biochemistry and Technology.* 4th ed., Studies in Inorganic Chemistry 10, Elsevier, Amsterdam, 1990, p. 428.
5. H. R. Allcock, in Inorganic and Organometallic Polymers, ASC Symposium Series 360, American Chemical Society, Washington, DC, 1988, p. 250.
6. H. R. Penton, in Inorganic and Organometallic Polymers, ASC Symp. Ser., Vol. 360, 1988, p. 277.
7. C. H. Allen, *Chem. Eng. News,* **70,** 45 (1992).
8. W. Allen, in *The Science and Technology of Fire Resistant Materials,* D. M. Macaione, Ed., Proceedings of 35th Sagamore Army Materials Research Conference, Plymouth, Massachusetts, Sept. 1992, p. 293.
9. Y. P. Belyaev, M. S. Trizno, and A. F. Nikolaev, *Plast. Massy,* **5,** 77 (1974).
10. L. A. Alekseenko, V. V. Kireev, and D. F. Kutepov, *Plast. Massy,* **11,** 13 (1978).
11. E. Devadoss, *J. Appl. Polym. Sci.,* **28,** 921 (1983).
12. D. Kumar, G. M. Fohlen, and J. A. Parker, *Macromolecules,* **16,** 1250 (1983).
13. D. Kumar, G. M. Fohlen, and J. A. Parker, *J. Polym. Sci., Polym. Chem. Ed.,* **21,** 3155 (1983).
14. D. Kumar, G. M. Fohlen, and J. A. Parker, *J. Polym. Sci., Polym. Chem. Ed.,* **22,** 927 (1984).
15. D. Kumar, G. M. Fohlen, and J. A. Parker, *J. Polym. Sci., Chem. Ed.,* **24,** 2415 (1984).
16. E. S. Oganes'an, V. F. Klusevich, A. S. Bukin, G. I. Martysheva, and D. H. Kulev, *Plast. Massy,* **6,** 62 (1991).
17. M. P. Prigozhina, L. G. Komarova, and A. L. Rusanov, *Plast. Massy,* **1,** 38 (1992).
18. M. D. Bezoari, U.S. Pat. US4745206 (1986) (to the Dow Chemical Co., Midland, MI).
19. D. Lin-Vien, N. B. Colthup, W. G. Fateley, and J. G. Grasselli, *The Handbook of Infrared and Raman Characteristic Frequencies of Organic Molecules,* Academic Press, Boston, 1991.
20. L. C. Thomas, *Interpretation of the Infrared Spectra of Organophosphorus Compounds,* Heyden, London, 1974.
21. R. A. Show, B. W. Fitzsimmons, and B. C. Smith, *Chem. Rev.,* **62,** 247 (1962).
22. B. W. Fitzsimmons and R. A. Shaw, *J. Chem. Soc.,* 1735 (1964).
23. B. W. Fitzsimmons, C. Hewlett, and R. A. Shaw, *J. Chem. Soc.,* 4459 (1964).

24. B. W. Fitzsimmons, C. Hewlett, and R. A. Shaw, *J. Chem. Soc.,* 7432 (1965).
25. H. R. Allcock and R. L. Kugel, *Inorg. Chem.,* **5,** 1016 (1966).
26. H. R. Allcock, R. L. Kugel, and K. J. Valan, *Inorg. Chem.,* **5,** 1709 (1966).
27. I. C. McNeill, in *Development in Polymer Degradation,* Vol. 1, N. Grassie, Ed., Applied Science Publishers, 1977, p. 43.
28. I. C. McNeill and A. Rincorn, *Poly. Deg. Stab.,* **24,** 59 (1989).
29. H. R. Allcock and R. J. Best, *Can. J. Chem.,* **42,** 447 (1964).
30. H. R. Allcock, G. S. McDonnell, and J. L. Desorcie, *Inorg. Chem.,* **29,** 3839 (1990).
31. H. R. Allcock and M. L. Turner, *Macromolecules,* **26,** 3 (1993).
32. W. T. Ferrar, F. V. DiStefano, and H. R. Allcock, *Macromolecules,* **13,** 1345 (1980).
33. E. Fitzer, K. Mueller, and W. Schaefer, in *Chemistry and Physics of Carbon, A Series of Advances,* Vol. 7, P. L. Walker Jr., Ed., Marcel Dekker, New York, 1971, p. 231.
34. T. N. Miller and A. A. Vitola, *Inorganic Compounds of Phosphorus and Nitrogen,* Zinatne, Riga, 1986, Chap. 8 (in Russian).